

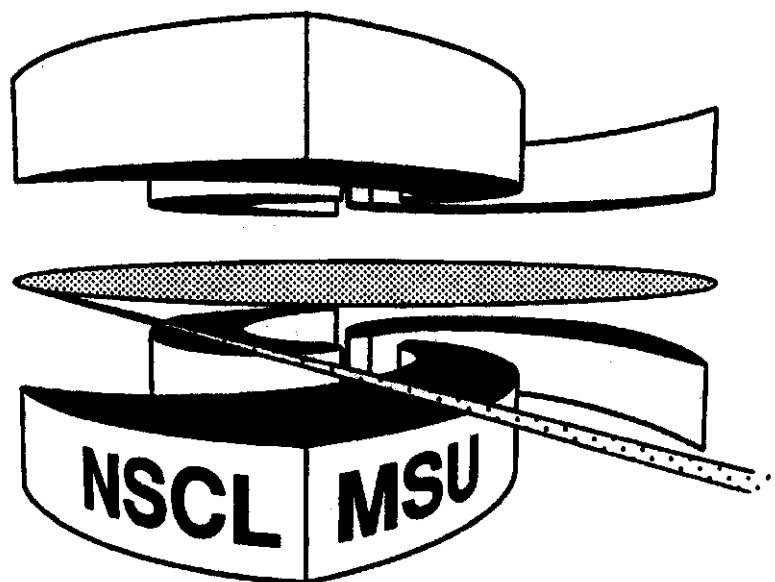


Michigan State University

National Superconducting Cyclotron Laboratory

n-n CORRELATIONS WITH EXOTIC NUCLEI

**A. GALONSKY, K. IEKI, D. SACKETT, J.J. KRUSE, W.G. LYNCH,
D.J. MORRISSEY, N.A. ORR, B.M. SHERRILL, J. WANG,
J.A. WINGER, P. ZECHER, F. DEÁK, Á. HORVÁTH, Á. KISS, Z.
SERES, J.J. KOLATA, R.E. WARNER, and D.L. HUMPHREY**



Won't you please share this preprint with your local colleagues.

n-n **CORRELATIONS WITH EXOTIC NUCLEI**

A. GALONSKY
*NSCL and Physics Department, Michigan State University
East Lansing, MI 48824, U.S.A.*

K. IEKI
*Department of Physics, Rikkyo University
3-34-IToshima, Tokyo 171 Japan*

D. SACKETT, J. J. KRUSE, W.G. LYNCH, D. J. MORRISSEY, N. A. ORR, B. M. SHERRILL, J. WANG, J. A. WINGER, P. ZECHER
*NSCL and Physics Department, Michigan State University
East Lansing, MI 48824, U.S.A.*

F. DEÁK, A. HORVÁTH, Á. KISS
*Department of Atomic Physics, Eötvös University
Puskinutca 5-7, H-1088, Budapest 8, Hungary*

Z. SERES
*KFKI Res. Inst. for Particle and Nuclear Physics of the Hungarian Academy of Sciences
H-1525 Budapest 114, Hungary*

J. J. KOLATA
*Department of Physics, University of Notre Dame
Notre Dame, IN 46556, USA.*

R. E. WARNER
*Department of Physics, Oberlin College
Oberlin, OH 44074, U.S.A.*

D. L. HUMPHREY
*Department of Physics, W. Kentucky University
Bowling Green, KY 42101 USA.*

ABSTRACT

A kinematically complete measurement of the Coabmb dissociation of ^{11}Li into $^9\text{Li} + 2n$ by a Pb target was made for ^{11}Li excitation energies up to ~ 1.5 MeV. The ^9Li velocity is greater than the average neutron velocity, indicating Coulomb acceleration of the ^9Li by the Pb nucleus and, therefore, a prompt decay rather than a soft dipole resonance for the breakup process.

The n-n momentum and angle correlations show no evidence for a dineutron in the ground state of ^{11}Li .

A brief discussion is given of two neutron walls under construction and of the problems of neutron spectroscopy with large detectors.

1. Introduction

Webster's dictionary says that something exotic is foreign or unfamiliar. There have been so many papers written about ^{11}Li in the last few years that, at least for some of us, ^{11}Li now seems more like an old friend than an unfamiliar nucleus. Nevertheless, in this paper ^{11}Li is taken as the archetypal exotic nucleus--a light, neutron-dripline nucleus that may be viewed as a core (^9Li) plus two neutrons. The same statements can be made about the dripline nuclei ^8He (^6He core) and ^{14}Be (^{12}Be core) and about ^6He (α -particle core). In all four nuclei the pairs -- core plus neutron and neutron plus neutron -- do not bind, but the three-body system is bound. It has been suggested that the neutrons in these nuclei form a bound dineutron.^{1,2} In any case, experimental information on the correlation between the neutrons would contribute to our understanding of the structure of these nuclei.

In principle, any interaction of ^{11}Li , even elastic scattering,³ will be sensitive to its ground-state wave function, but some interactions will be more sensitive than others. In the experiment we performed^{4,5} ^{11}Li was dissociated by photon absorption into $^9\text{Li} + n + n$, and we detected both neutrons. A ^{11}Li target being unattainable, two ingenious developments were used--the radioactive beam facility⁶ at Michigan State University and the method of equivalent photons.^{7,8} ^{11}Li became the projectile, and the electric field of a Pb target nucleus was the photon source. Although the photon spectrum is calculable,⁸ we have no control over the energy of the photon absorbed in a given event. E_γ is discovered only after a complete kinematics analysis of the event. That analysis yields the decay energy E_d , and then

$$E_\gamma = E_d + S_{2n}, \quad (1)$$

where S_{2n} is the two-neutron separation energy, 0.31 MeV⁹ in ^{11}Li . Each event is transformed back into the ^{11}Li rest frame, where various histograms, including those for n - n correlations, may be constructed.

The measured correlations are of the final state, not the initial (ground) state. To deduce a ground-state correlation we should know the transition operator and the final state wavefunction. A very appealing model of the electromagnetic dissociation developed,^{2,10,11} the so-called soft dipole model. In this model ^{11}Li is excited by E1 photon absorption into an electric dipole resonance similar to the giant dipole resonance.

In the giant dipole resonance the photon drives all the protons against all the neutrons in a nucleus. From the systematics on restoring force and inertia, the resonant energy in ^{11}Li would be expected to be ~ 25 MeV. The soft dipole resonance is another collective resonance in which the restoring force on the oscillating protons is provided by the two halo neutrons. Schematics of these two electric dipole resonances are shown in Fig. 1. The latter resonance should occur only when the valence neutrons are so lightly bound that they form a halo around the charged core.

The dipole strength function is obtained from the equation

$$\text{Photon Absorption } \sigma = (\text{E1 Strength Function}) * (\text{Virtual Photon Spectrum.}) \quad (2)$$

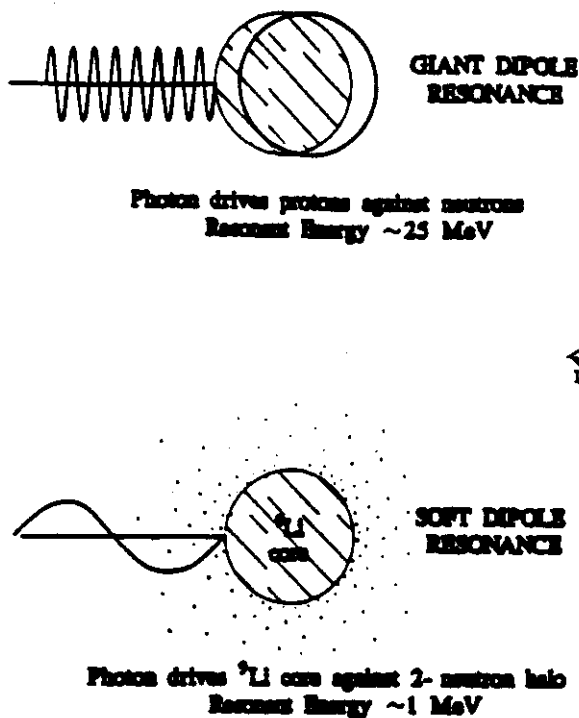


Fig. 1. The mechanics of the giant dipole resonance and the proposed soft dipole resonance.

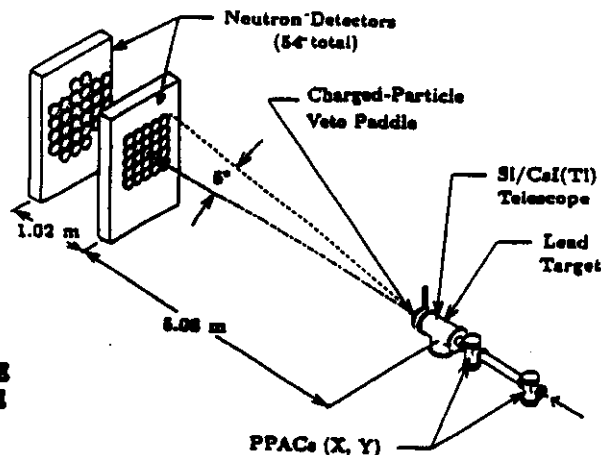


Fig. 2: Detector setup. The ^{11}Li beam enters from the lower right.

2. The Experiment

The complete kinematics were measured with the apparatus illustrated in Fig 2. The beam was incident from the lower right at an energy of 30 MeV/nucleon. Each ^{11}Li projectile had already generated a time-of-flight start signal in a scintillator. From its signal in the ΔE Si detector, we could determine its kinetic energy, and from the two PPAC (x,y) signals its direction. Energy and direction of the ^9Li decay fragment were measured with the Si/CsI telescope; the Si had 16x and 16y strips, effectively defining 256 pixels of angular width 1.2° . Energy and direction of each neutron were determined from flight time and neutron detector (liquid scintillator) position.

3. Soft Dipole Resonance

3.1. $E1$ Strength Function

The decay energy spectrum is shown in the left half of Fig. 3. In the right half is the deduced electric dipole strength function. To compare a dipole strength function with our data, we must multiply the strength function by the virtual photon spectrum (Eq. 2) and by our detector response function. Because the angular acceptance of the neutron array is only 5° , the response is a rapidly decreasing function of decay energy. A neutron emitted with 0.3 MeV and at 90° in the ^{11}Li rest frame, for example, will have an angle of $\sqrt{0.3/30} = 0.1$ or 6° in the laboratory; it will miss the neutron array. When the solid curve in the

right half of Fig. 3 was Monte-Carloed through our detector response function (and the photon spectrum), it produced the solid curve that fits our data so well in the left half. The solid curve in the left half is the dipole strength function determined by our data. A theoretical model that produces a dipole strength function in agreement with this curve is in agreement with our data.

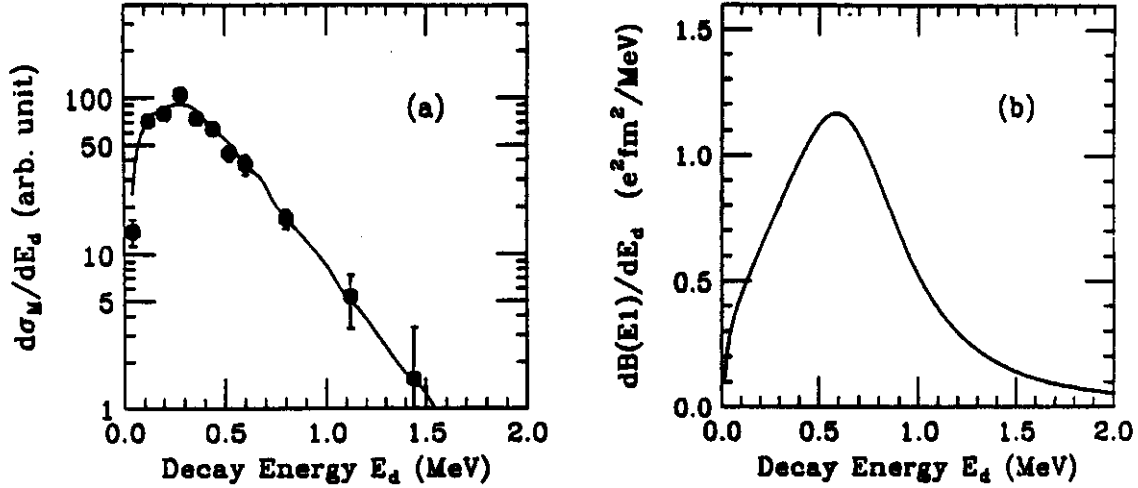


Fig. 3: (a) The measured decay energy spectrum of $^{11}\text{Li} \rightarrow ^9\text{Li} + n + n$. (b) The corresponding electric dipole strength function. The solid curve below results from a Breit-Wigner resonance function with $E_{\text{res}} = 0.7$ MeV and $\Gamma = 0.8$ MeV. This curve, with the virtual photon spectrum and the detector response function, produced the data-fitting curve in (a).

To obtain the fit that is shown we assumed a Breit-Wigner resonance shape and searched on its two parameters--resonance energy and width. The results were $E_d=0.7$ MeV ($E_x=E_d+S_{2n}\cong 1.0$ MeV) and $\Gamma=0.8$ MeV. It is instructive to compute the times corresponding to these energies. If our resonance represents the soft dipole resonance, the period of oscillation of the ^9Li core in the two-neutron halo may be obtained as follows:

$$E_x = \hbar\omega = \hbar 2\pi/T; T=2\pi\hbar c/E_x c \cong 1250 \text{ fm}/c \quad (3)$$

From the width of the state we get its lifetime:

$$\Gamma\tau = \hbar; \tau = \hbar c/\Gamma c = 200/0.8 = 250 \text{ fm}/c \quad (4)$$

Therefore, the state lives for only 1/5 of a oscillation, on average. Such a short lifetime does not support the picture of a core oscillating back and forth in the halo.

3.2. Post-Breakup Coulomb Acceleration

An observation that was not expected in the experiment is shown in the left half of Fig. 4. The ^9Li velocity is systematically higher than the average neutron velocity. To check for a possible instrumental bias we ran a computer simulation of un-accelerated

events and got the histogram in the figure. It is symmetrical and centered on zero. Of course, our fragment and neutron velocities were measured by different means, the fragment by the energy deposited in a calibrated CsI scintillator, the neutron by its flight time. Although our estimates of the systematic error in each of the two measurements could not account for the observed velocity difference, we were able to construct an experimental check, as illustrated in the right half of Fig. 4. There we compare the initial center-of-mass velocity, ($\approx {}^{11}\text{Li}$ velocity), with the final CM velocity. Since the latter value depends mostly on the ${}^9\text{Li}$ velocity, which comes from energy deposition, and the former (and the neutron velocity) comes from time-of-flight measurement, the almost perfect centering of this distribution is reassuring. The width of the distribution is a measure of our instrumental velocity difference resolution.

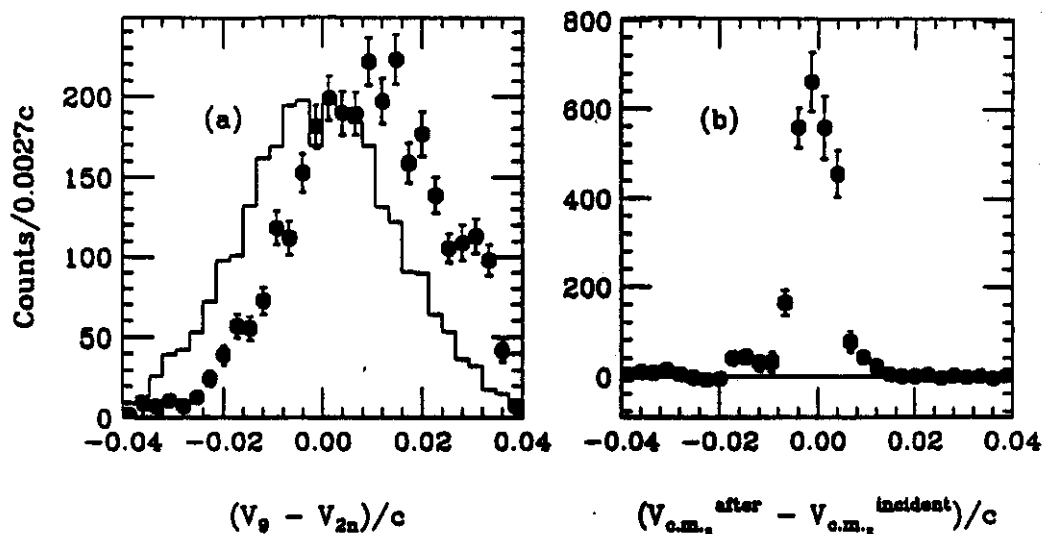


Fig. 4. (a) The spectrum for the velocity difference $V_9 = V_{2n}$, where V_{2n} is the average velocity of the two detected neutrons. The histogram is the result of a Monte-Carlo simulation assuming no Coulomb-acceleration effects. (b) The spectrum for the longitudinal component of the center-of-mass velocity before breakup subtracted from the center-of-mass velocity after breakup.

We have no choice but to take the observed velocity difference seriously and try to interpret it. One possible interpretation is illustrated by the simplified sketch in Fig. 5. This shows that if the lifetime of the excited ${}^{11}\text{Li}$ is short enough, break-up will occur while the Li is still high on the Coulomb hill. ${}^9\text{Li}$ will receive a Coulomb acceleration, and the neutrons will not. We can work this idea backwards from the measured value of $V_9 - V_{2n}$. That value determines the Coulomb energy, which determines r in Fig. 5, and r determines τ , the result being $\tau \sim 60 \text{ fm/c}$. From the width of the

"resonance" we deduced a τ of 250 fm/c. More doubt is cast on the existence of a resonant state. The peak in Fig. 3 looks like a resonance, but an excitation function must rise from zero at threshold and, because of a sum rule, eventually come down again. The Coulomb acceleration method of lifetime determination is independent of whether or not there is a soft-dipole resonance, and, of course, 60 fm/c is only 5% of the 1250 fm/c oscillation period for a soft-dipole resonance at $E_x = 1 \text{ MeV}$. We conclude that we have observed a direct break-up of ${}^{11}\text{Li}$, rather than a soft-dipole resonance.

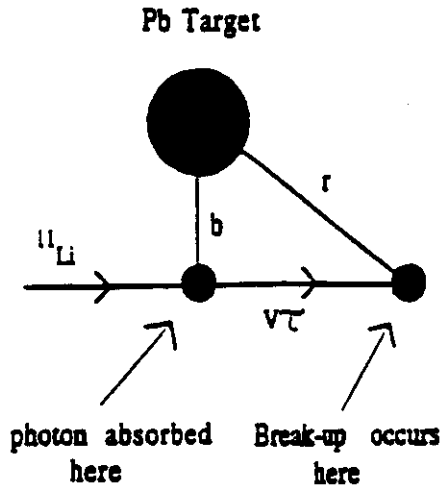


Fig. 5: A schematic view of a ^{11}Li breakup. The average impact parameter is b . The distance from the Pb nucleus to the breakup point is denoted by r . v is the beam velocity and τ is the meanlife of the excited ^{11}Li .

requirement would have been met very well because the electric field of the Pb nucleus would have been a flattened pancake as seen by the ^{11}Li . With an impact parameter of 10-20 fm and a speed of c , the collision time could have been less than 1 fm/c. A halo neutron has radius ~ 3 fm. With momentum 18 MeV/c, its speed is only $0.02c$, and its orbital period ~ 900 fm/c, which is \gg the collision time. At 28 MeV/nucleon $v = c/4$, however, there is almost no flattening. Photon absorption occurs over a time of $\sim (30 \text{ fm})/(c/4) = 120$ fm/c. As this is somewhat less than the orbital period, the second requirement is somewhat satisfied. We can expect, but not be certain, that a dineutron in the ground state would show itself in the final state. With that expectation, we look for evidence for a dineutron in our data.

4.1 Momentum Distributions

If the Coulomb dissociation is indeed both gentle and sudden, a dineutron structure in the ground state results in a two-body breakup in the first instance. The kinematics of the breakup are reflected in the momentum spectrum of the ^9Li . For a given value of E_d , two-body decay gives a spectrum with all ^9Li at the maximum possible value. When summed over the E_d values in this experiment, Fig. 3, a continuum results, but it is a maximized continuum, it is the solid histogram of Fig. 6a. The data are not fitted by this model, but they are fitted by the two other models shown--a three-body phase-space model and the three-body hyperspherical-harmonic direct-breakup model.¹⁶ In the Hyperspherical-harmonic model the angular effects of the $\ell = 1$ photon absorption are included. The same three models are compared with the data on the momentum distribution of a single neutron in Fig. 6b. Again, the three-body models agree with the data. but the dineutron model predicts a spectrum beyond the measured spectrum.

4. The Dineutron in ^{11}Li

With a direct transition to continuum states, the equivalent photon method could be a very good way to look at the ground-state structure of ^{11}Li . There are two requirements: 1) the momentum of the absorbed photon should not significantly perturb the motion of the ^9Li core or of either neutron, it should be a gentle perturbation, and 2) the photon absorption process should take place so quickly that the positions of the three constituents are not significantly changed, it should be a sudden absorption. If these requirements are met, no theory is required to see the $n-n$ ground-state correlation in the final state. A look at parts (a) and (b) of Fig. 6 tells us that the first requirement is met, because a typical ^9Li momentum is about 30 MeV/c and a typical neutron momentum is about 18 MeV/c, whereas Fig. 3 gives $p_\gamma \leq 1$ MeV/c. If our beam velocity had been relativistic, the second

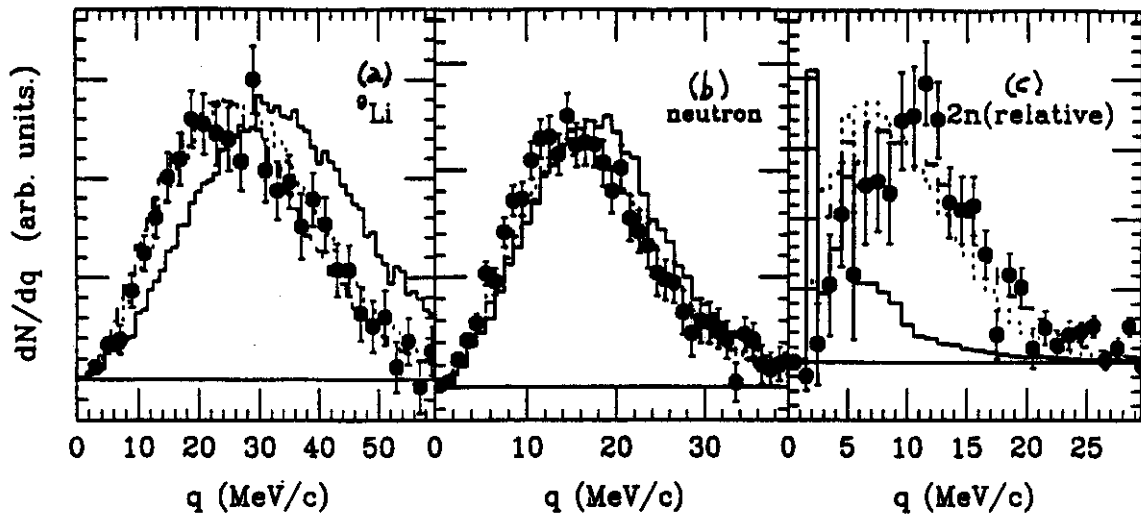


Fig. 6 Momentum spectra of ${}^9\text{Li}$ fragments, single neutrons, and of one neutron relative to the center-of-mass of the two neutrons. The points are from our experiment. The histograms are Monte-Carlo simulations of three decay models: dashed--standard 3-body phase space, dotted--3-body hyperspherical-harmonic (Ref. 16), solid--2-body decay into ${}^9\text{Li}$ and a dineutron.

Finally, in Fig. 6c we look at the $n - n$ relative momentum spectrum, i.e., the spectrum of the momentum of one neutron with respect to the center-of-mass of the two neutrons. With an ideal neutron detector all the events in the dineutron model would have $q = 0$, and that would be the case for all values of E_d . Unlike the ${}^9\text{Li}$ and n spectra, there is no dilution here of the dineutron effect when, for statistical accuracy, events with a range of E_d values are summed together. The response of our detector changes that, but there is still a large discrepancy between the spectral shapes of the data and the prediction. The two three-body models agree with the data. No $n-n$ final state interaction was put into the model calculations of Fig. 6.

4.2 $n - n$ Angle Distribution

The dineutron model makes another prediction which is independent of E_d --that the angle θ between the two neutrons is zero, $\cos \theta = 1.0$. The detector response smooths the prediction but still leaves a strong peak at $\cos \theta = 1$. In Fig. 7 that peak goes off scale beyond 2,000--more than ten times the value in our data. Again, the two other models more-or-less equally agree with the data.

4.3 Comparison with Others Results

Although our experiment gave no evidence in favor of the existence of a dineutron in ^{11}Li , there are at least two reports that do give such evidence. In one,¹⁴ average values of ^9Li and of single-neutron momentum distributions were used to deduce a value for the

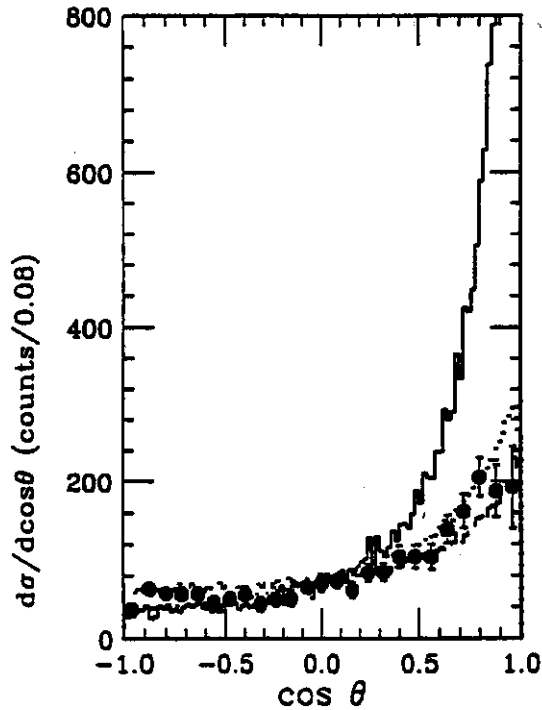


Fig. 7 Angle distribution of the two neutrons when ^{11}Li decays into $^9\text{Li} + n + n$. The angle between the neutrons is θ . The points are from our experiment. The histograms are Monte-Carlo simulations of three decay models; dashed--standard 3-body phase space, dotted--3-body hyperspherical-harmonic (Ref. 16), solid--2-body. The last one rises above 2,000 at $\cos \theta = 1$.

experimental difficulties with neutron detection. In order to maintain a reasonable energy resolution, the detector thickness must be small, resulting in a detection efficiency significantly < 1 , typically 0.1. In a two--neutron experiment the efficiency is the 0.01. And with a "beam" of an exotic nucleus the intensity is far below the 1.0 particle μA ($6 \times 10^{12}/\text{s}$) that was once standard in a nuclear physics experiment. Our ^{11}Li intensity was $< 6 \times 10^2/\text{s}$. A large neutron detector, such as the 54-can array in Fig. 2, partially compensates for this deficiency.

We are building a pair of neutron walls, each consisting of 25 long glass cells filled with NE213 liquid scintillator and having photo tubes at the ends. This will give us a factor of 10 increase in the volume of scintillator but with only 100 photo tubes rather than 540. The 2 m x 2 m wall area will give us 3 times the angular acceptance and, therefore, reasonable efficiency for events with 9 times the decay energy. A computer photograph of

average of $\cos \theta$, and the result was that it was, with a significant statistical error, greater than 1, i.e., it was consistent with $\theta = 0$. The other¹⁵ reports on a complete-kinematics experiment similar to decay into ^9Li and a dineutron ours, the main differences being that the beam energy was 43 MeV/u (compared to our 28 MeV/u), the neutron angular acceptance was greater, and there was no neutron/ γ -ray pulse-shape discrimination. Two related pieces of evidence are given in favor of a "modified" (i.e., at least some) dineutron model. First, partitioning of the decay energy into kinetic energy of the $^9\text{Li} - n^2$ system and internal energy of the n^2 system strongly favored the former, whereas the two energies were about equal in our experiment. Zero internal energy of the n^2 system is equivalent to what we have taken as the dineutron model. And second, their $n - n$ relative energy spectrum includes a narrow peak at 50 keV, equivalent to $q = 5$ MeV/c in Fig. 6c.

5. Future Plans--the Neutron Wall

The discrepancy between our experiment and that of Shimoura et al.¹⁵ is not too surprising if one is aware of the

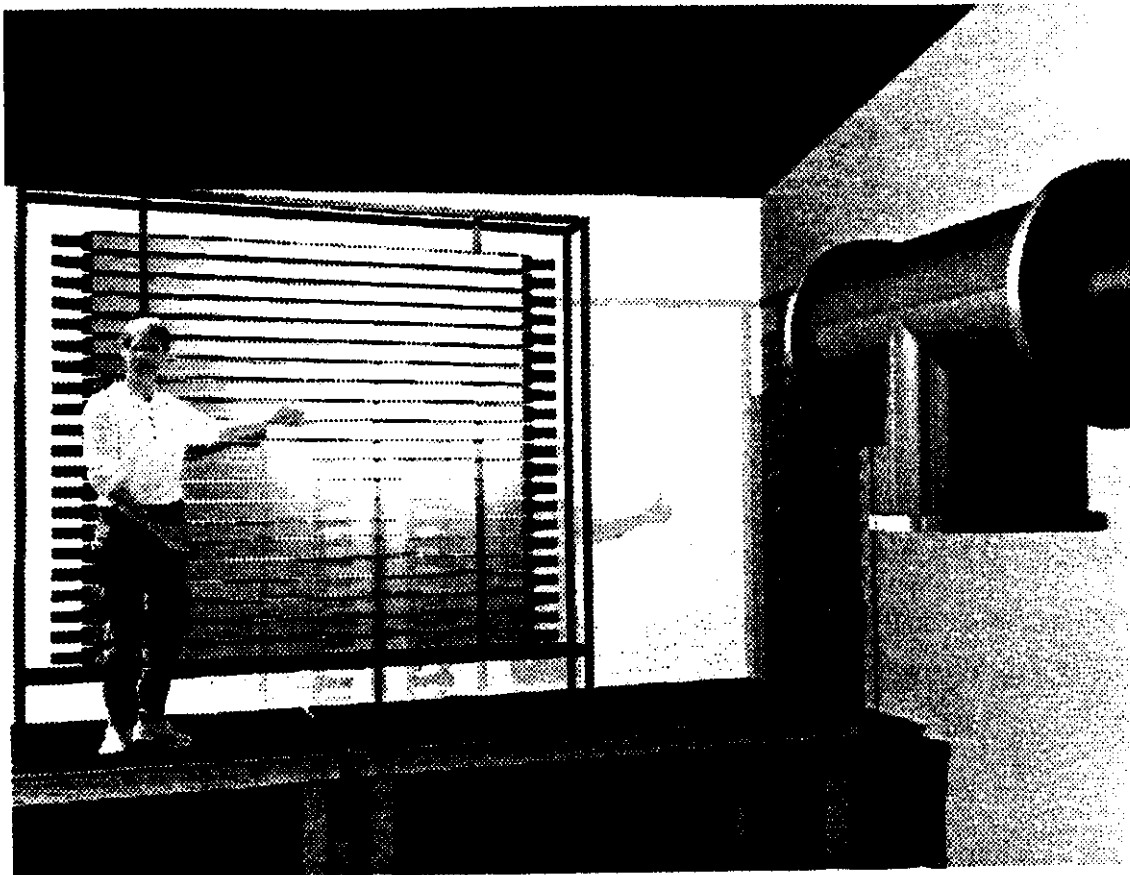


Fig. 8. A computer photograph of one of the neutron walls under construction at Michigan State University. The human model, Mr. P. Zecher, one of the coauthors of this report, is almost 2-m tall.

the wall is shown in Fig. 8. The size may be judged from the human model, Mr. P. Zecher, a co-author of this report who is almost 2-m tall.

Even with these walls there will be two experimental problems in measuring $n - n$ correlations--cross-talk and scattering. By cross-talk we mean a pair of scatterings or interactions whereby one neutron produces pulses in two of the glass cells thereby mimicking a true 2-neutron event. For example, the first interaction could be



and the second, $n' - p$ elastic scattering. To reduce the number of such events we plan to run our experiments at a low enough beam energy and with a high enough pulse-height threshold that almost all of our detection efficiency will come from $n - p$ elastic scattering and almost none from $n - {}^{12}\text{C}$ interactions. This will allow us to use the 2-body kinematics of $n - p$ scattering to test each event for possible cross-talk. The test will be made with a computer simulation program (written by Mr. J. Wang, co-author of this paper) that allows for the instrumental resolutions of pulse height, x and y positions on the wall, and time

determination. As a check on the program we will expose the walls to neutrons from the ${}^7\text{Li}$ (p,n) reaction. All 2-cell events from this 1-neutron reaction will be cross-talk events. To first order the simulation program should identify all of them as such. However, there is another effect--scattering--that defeats this goal and that causes other difficulties. In-scattering is an ancient problem in neutron physics. It refers to neutrons that arrive at the detector after scattering from the floor, the walls or some other part of the surroundings. The detector, not being direction sensitive, accepts this neutron and assigns it a rather low energy because of its long flight time. The traditional solution is to measure the in-scattering and subtract it. To do this a shadow-bar is inserted in the path between source and detector, allowing only in-scattered neutrons to reach the detector. With either an array of detectors or a wall, out-scattering makes it impossible for this kind of detector to be perfect. An out-scattered neutron is one which enters a part of the detector, is scattered without making a detectable light pulse, and arrives at another part of the detector where it does make a big enough light pulse. It is thereby assigned an incorrect position and an incorrect (too low) velocity. The scattering material could be the detector housing or the carbon and hydrogen of the scintillator itself. Even with the lightest housing the effect is still present. Perhaps the only way to account for the effects of out-scattering is to feed any model of the produced neutron distributions through a computer simulation of the neutron detector.

Acknowledgements

We wish to gratefully acknowledge the support of the U.S. National Science Foundation under Grant Numbers INT91-13997 and PHY92-14992 and of the Hungarian Academy of Sciences.

References

1. A. B. Migdal, *Yad. Fiz.* 16 (1972) 427; English translation *Sov. J. Nucl. Phys.* 16 (1973) 238.
2. P. G. Hansen and B. Jonson, *Europhys. Lett.* 4 (1987) 409.
3. I. J. Thompson, J. S. Al-Khalili, J. A. Tostevin and J. M. Bang, *Phys. Rev. C* 47 (1993) R1364.
4. K. Ieki, D. Sackett, A. Galonsky, C. A. Bertulani, J. J. Kruse, W. G. Lynch, D. J. Morrissey, N. A. Orr, H. Schultz, B. M. Sherrill, A. Sustich, J. A. Winger, F. Deák, Á. Horváth, Á. Kiss, Z. Seres, J. J. Kolata, R. E. Warner and D. L. Humphrey, *Phys. Rev. Lett.* 70 (1993) 730.
5. E. Sackett, K. Ieki, A. Galonsky, C. A. Bertulani, H. Esbensen, J. J. Kruse, W. G. Lynch, D. J. Morrissey, N. A. Orr, B. M. Sherrill, H. Schulz, A. Sustich, J. A. Winger, F. Deák, Á. Horváth, Á. Kiss, Z. Seres, J. J. Kolata, R. E. Warner and D. L. Humphrey, *Phys. Rev. C* 48 (1993) 118.
6. B. M. Sherrill, D. J. Morrissey, J. A. Nolen and J. A. Winger, *Nucl. Instrum. Methods B* 56/57 (1991) 1106.

7. G. Baur, C. A. Bertulani and H. Rebel, *Nucl. Phys.* **A458**, (1986) 188.
8. C. A. Bertulani and G. Baur, *Phys. Rep.* **163**, (1988) 299.
9. G. Audi and A. H. Wapstra, *Nucl. Phys.* **A565** (1993) 66.
10. T. Kobayashi, S. Shimoura, I. Tanihata, K. Katori, K. Matsuta, T. Minamisono, K. Sugimoto, W. Muller, D. L. Olson, T. J. M. Symons and H. Wieman, *Phys. Lett.* **B232**, (1989) 51.
11. K. Ikeda, *Nucl. Phys.* **A538**, (1992) 355c.
12. C. A. Bertulani, G. Baur and m. S. Hussein, *Nucl. Phys.* **A526**, (1991) 751.
13. H. Esbensen and G. F. Bertsch, *Nucl. Phys.* **A542**, (1992) 310.
14. I. Tanihata, T. Kobayashi, T. Suzuki, K. Yoshida, S. Shimoura, K. Sugimoto, K. Matsuta, T. Minamisono, W. Christie, D. Olson and J. Wieman, *Phys. Lett.* **B 287**, (1992) 307.
15. S. Shimoura, T. Nakamura, M. Ishihara, N. Inabe, T. Kobayashi, T. Kubo, R. H. Siemssen, I. Tanihata and Y. Watanabe, preprint.
16. L. V. Chulkov, B. Jonson and M. V. Zhukov, *Europhys. Lett.* **24**, (1993) 171.